XLI CILAMCE
XLI Ibero-Latin American Congress on Computational Methods in Engineering
16-19 November, 2020 FOZ DO IGUAÇU PARANÁ – BRAZIL

Numerical modeling of fracture propagation using continuum damage and cohesive crack models

Ilames J. G. Moraes[1,2], Rafael O. A. Abreu[1,2], Cristian Mejia[2], Deane Roehl[1,2]

[1]*Dept. of Civil and Environmental Engineering, Pontifical Catholic University*
Marquês de São Vicente st, Gávea., 22451-000, Rio de Janeiro, Brazil
ilamesjordan@tecgraf.puc-rio.br, radaeloabreu@tecgraf.puc-rio.br, deane@tecgraf.puc-rio.br
[2]*Tecgraf Institute, Pontifical Catholic University*
Marquês de São Vicente st, Gávea., 22451-000, Rio de Janeiro, Brazil
crisms@tecgraf.puc-rio.br

Abstract. Damage mechanics is a branch of the inelastic theory, which is concerned with the impact of the growth of microvoids or microcracks in solids. From a structural point of view, a solid body loses stiffness as a consequence of damage evolution. This work aims at understanding fracture propagation in quasi-brittle materials, considering continuum damage and cohesive crack models. The cohesive zone model and isotropic damage model are implemented into the in-house framework GeMA. In the finite element context, modeling of the material degradation process is a challenging task due to the occurrence of critical points and convergence problems in the global solution. Therefore, robust continuation methods are required to overcome this obstacle. Regularization techniques are applied in the isotropic damage models to reduce the pathological sensitivity of the solution to the finite element size. Numerical simulations illustrate the ability and limitations of the proposed models to simulate fracture propagation. Additionally, various damage criteria and evolution laws proposed by several authors are adopted to evaluate the impact of the model on the global behavior. The results indicate that continuum damage and cohesive zone modeling are crucial tools to provide realistic responses related to fracture processes.

Keywords: Isotropic damage model, Cohesive zone model, Fracture propagation, Quasi-brittle materials.

1 Introduction

The fracture propagation in quasi-brittle materials, such as concrete and rock, is preceded by the development of a zone with microcracks (fracture process zone) that is still capable of transmitting forces (Van Mier [1], Wight and MacGregor [2]). The coalescence of these microcracks and microvoids leads to the formation of macrocrack, characterizing the completely damaged zone, where forces are no longer transmitted. In this sense, several constitutive models have been proposed to model this phenomenon. Thereby, damage mechanics is a branch of the inelastic theory that studies the impact of the growth of discontinuities in solids. In general, the damage process is irreversible and can be associated with creep, fatigue, or plastic deformation. From a structural point of view, stiffness loss is an effect of the damage evolution. In 1958, the damage mechanics was initially described by Katchanov to explain the fracture process in creeping metals (Lemaitre [3]). Afterwards, Lemaitre [3] presented a formalism considering the thermodynamic perspective. Several initiation criteria and damage evolution laws have been studied by distinct authors, such as Mazars [4], Kurumatani et al. [5], Oliver et al. [6], and Simo and Ju [9], to assess the stiffness degradation process.

Another constitutive model capable of describing the fracture propagation process is the cohesive zone model. This model avoids the stress singularity at the crack tip (Nguyen [10]). Moreover, the cohesive constitutive model relates the cohesive tractions on the crack surface to the crack opening. In the finite element method, zero-thickness interface elements with a cohesive model are placed between solid elements to describe the nucleation and fracture propagation (Mejia et al. [11]).

This work aims at studying the description of the fracture process using the isotropic damage and cohesive zone models. These constitutive models are implemented into the in-house finite element framework GeMA. Both constitutive models are adopted to reproduce fracture propagation in quasi-brittle materials. In the finite element context, the global solution of problems involving the material degradation process presents critical points and convergence problems. To overcome these obstacles, robust continuation methods are required. For damage models, several techniques are usually adopted to reduce the mesh dependence, such as the non-local model (De Vree et al. [12]), a combination of a non-local model and a mesh-adaptive technique (De-Pouplana and Oñate [7]), and microplane model (Bažant et al. [13] and Caner and Bažant [14]). This work adopts the regularization technique based on the characteristic length, calculated according to the area of each finite element, as presented by Kurumatani et al. [5]. Also, several damage criteria and laws of evolution proposed by numerous authors are adopted in this work to assess the effects on global behavior.

2 Isotropic damage model

The fracture initiation and propagation in quasi-brittle materials present a series of factors that hinder its modeling due to their heterogeneity, anisotropy, and nonlinear behavior. The isotropic damage model is a simple model capable of describing gradual stiffness loss of the material. The damage evolution of this sort of model is measured using scalar variables in the interval [0,1]. It is important to emphasize that the damage variable does not affect Poisson's ratio. The behavior of the damaged material is represented by a simple stiffness correction of the undamaged material, as expressed in eq. (1):

$$\boldsymbol{\sigma} = (1 - d)\boldsymbol{D}\colon \boldsymbol{\varepsilon}, \tag{1}$$

where d represents the damage variable, $\boldsymbol{D}$ is the constitutive tensor, and $\boldsymbol{\sigma}$ and $\boldsymbol{\varepsilon}$ are the stress and strain tensors, respectively.

In general, the damage loading function f is defined in terms of equivalent strain ε_{eq}. Furthermore, this function is analogous to yield functions according to the plasticity theory. Several damage initiation criteria are proposed to compute the equivalent strain. In section 2.1, some damage criteria will be discussed in more detail. Furthermore, the state variable r is updated according to the equivalent strain (Oliver et al. [6]):

$$f = \varepsilon_{eq} - r. \tag{2}$$

After damage initiation, the loading-unloading-reloading process is numerically reproduced by updating the damage variable r, as given by eq. (3) (Oliver et al. [6]):

$$r = max\left(r_0, \max_{\tau \le t} \varepsilon_{eq}(\tau)\right), \tag{3}$$

where t represents the current pseudo-time and the damage threshold r_0 is defined as the equivalent strain value for which the material damage starts.

Finally, the damage evolution law describes the material softening behavior. Distinct evolution laws are proposed in the literature, such as linear and exponential laws. In section 2.2, some damage evolution laws will be discussed.

2.1 Damage criteria

There are several damage initiation criteria to define the equivalent strain for quasi-brittle materials. This work adopts the strain norm, Mazars, and the modified von Mises criteria. The strain norm criterion is based on the energy norm of the strain tensor normalized with respect to Young's modulus E. For this criterion, the equivalent strain is defined as:

$$\varepsilon_{eq} = \sqrt{\frac{\boldsymbol{\varepsilon}\colon \boldsymbol{E}\colon \boldsymbol{\varepsilon}}{E}}, \tag{4}$$

Mazars [4] criterion is computed from the positive principal strains. Thus, this criterion presents better results in analyzes, where the hydrostatic strain is more significant than the shear strain (Moreira and Evangelista Junior [17]). The equivalent strain, according to Mazars [4], is defined as follows:

$$\varepsilon_{eq} = \sqrt{\sum_i \langle \varepsilon_i \rangle^2}\ , \tag{5}$$

where the subscript i indicates the i-th strain and $\langle \cdot \rangle$ are the McAuley brackets.

The modified von Mises criterion, proposed by De Vree et al. [12], is suitable for quasi-brittle, according to Kurumatani et al. [5]. Its mathematical definition is given by

$$\varepsilon_{eq} = \frac{\kappa - 1}{2\kappa(1 - 2\upsilon)} I_1 + \frac{1}{2\kappa}\sqrt{\left(\frac{\kappa - 1}{1 - 2\upsilon} I_1\right)^2 + \frac{12\kappa}{(1 + \upsilon)^2} J_2}\ , \tag{6}$$

where υ is the Poisson's ratio, κ is the ratio between tensile and compressive strength, I_1 is the first strain invariant, and J_2 is the second invariant of the strain deviatoric tensor. Figure 1 presents a schematic representation of these criteria.

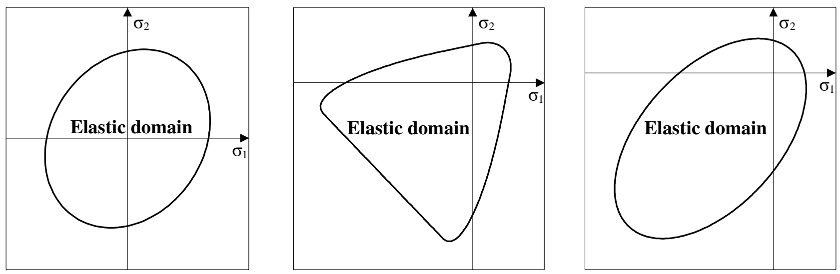

(a) (b) (c)

Figure 1. Biaxial failure envelope for (a) strain norm, (b) Mazars and (c) modified von Mises criteria

2.2 Damage evolution law

This work adopts the linear and exponential damage evolution laws. The linear law in eq. 7 controls the damage variable according to the state variable r, the damage threshold r_0 and the equivalent strain that leads to the fully damaged state r_{max}. Pohl et al. [15] presented a procedure to determine the failure strain, which is dependent on the finite element size. Thus, meshes with different element sizes have different values of r_{max}.

$$d = g(r) = \frac{r_{max}}{r}\frac{r - r_0}{r_{max} - r_0} \leq 1. \tag{7}$$

The exponential damage law proposed by Kurumatani et al. [5], defines the damage evolution in terms of the fracture energy, as follows

$$d = g(r) = 1 - \frac{r_0}{r} exp\left(-\frac{E r_0 l_{ch}}{G_f}(r - r_0)\right), \tag{8}$$

where G_f is the fracture energy, and l_{ch} is the characteristic length of the finite element. For quadrilateral finite elements, l_{ch} is the square root of the element area (Kurumatani et al. [5]).

3 Cohesive zone model

The cohesive zone model relates the tractions on the fracture surface $\tau = \{\tau_s \quad \tau_n\}$ to their relative displacement jump (separation) $\Delta = \{\Delta_s \quad \Delta_n\}$ (Nguyen [10]). The traction separation law for a linear elastic behavior is defined in eq. 9 (Mejia et al. [11]).

$$\begin{Bmatrix} \tau_s \\ \tau_n \end{Bmatrix} = \begin{bmatrix} k_s & 0 \\ 0 & k_n \end{bmatrix} \begin{Bmatrix} \Delta_s \\ \Delta_n \end{Bmatrix}, \tag{9}$$

where k_s and k_n are the normal and shear elastic stiffness, respectively. This work adopts a cohesive zone model with a linear softening law. This model assumes linear behavior up to the tensile strength, where the damage evolution starts. A quadratic damage initiation criterion is adopted (Mejia et al. [11]).

$$\left(\frac{\tau_s}{\tau_{s0}}\right)^2 + \left(\frac{\langle\tau_n\rangle}{\tau_{n0}}\right)^2 = 1, \tag{10}$$

where τ_{s0} and τ_{n0} represent the shear and normal strength. Figure 2 shows a typical traction-separation curve of a cohesive model. The post-critical regime represents the softening behavior that indicates the loss of material stiffness. The area under the curve represents the cohesive fracture energy.

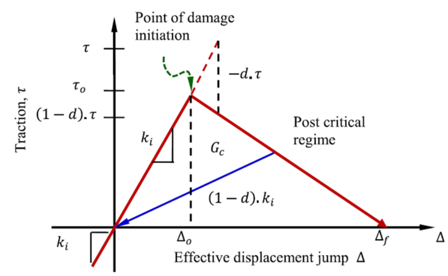

Figure 2. The typical response of the cohesive zone model

Furthermore, the tractions are evaluated using the scalar damage variable:

$$\begin{Bmatrix}\tau_s\\ \tau_n\end{Bmatrix} = \begin{bmatrix}(1-d)k_s & 0\\ 0 & (1-d)k_n\end{bmatrix}\begin{Bmatrix}\Delta_s\\ \Delta_n\end{Bmatrix}. \tag{11}$$

4 Numerical examples

The numerical examples developed in this work are L-shaped panels presented by Pohl et al. [15] and Winkler et al. [18] in plane stress condition. The analyzes were performed in GeMA (Geo Modeling Analysis), which is an in-house framework for multiphysics and multiscale analysis developed in Tecgraf/PUC-Rio Institute. The finite element plugin implemented in GeMA has several continuation methods to overcome the limit points, such as arc length control, displacement control, energy dissipation control, and combination methods proposed by Paullo Muñoz and Roehl [19]. In this work, the continuation method adopted was the dissipation of energy, presented by Gutiérrez [20]. Geometrical linearity is taken into account in all problems. For more details about GeMA, see Mendes et al. [21].

The first example considers the L-shaped panel presented by Pohl et al. [15]. The panel is discretized in two different meshes using bilinear quadrilateral elements with four integration points. The first mesh consists of 300 elements with an element size of 0.50 m (coarse mesh), while the second mesh consists of 7500 elements with 0.1m element size (refined mesh), as depicted in Fig. 3. The mechanical properties are $E = 10$ kN/m^2, $\upsilon = 0$ and $r_0 = 0.01$. For simulations considering a linear damage law, r_{max} is equal to 0.1 for the refined mesh and is equal to 0.02 for the coarse mesh.

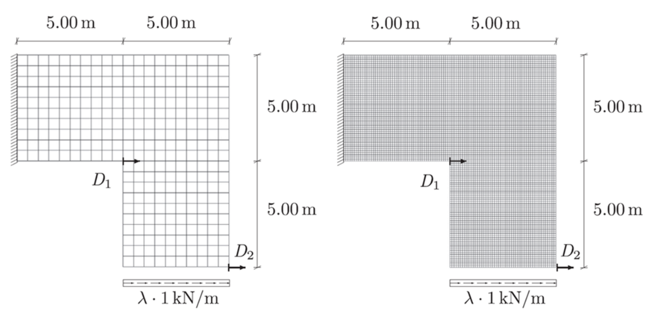

(a) b)

Figure 3. L-shaped panel (a) coarse mesh and (b) fine mesh (Pohl et al. [15])

Figure 4 shows the scalar damage variable at the end of the simulation. The red color indicates the completely damaged material, while the blue color represents the undamaged material. Figures 4a and 4c exhibit the numerical results obtained for the coarse mesh using the continuum damage and cohesive zone models, respectively. Figures 4b and 4d present the numerical results obtained for fine mesh using both models.

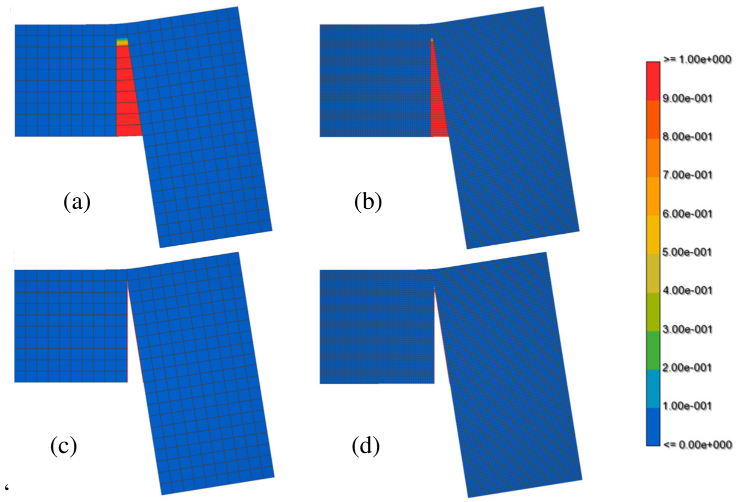

Figure 4. Deformed structure for the continuum damage modeling in (a) and (b), and the cohesive zone modeling in (c) and (d) using coarse and fine meshes.

Figures 5a and 5b present the load-displacement curves obtained for the coarse and fine meshes, respectively, and the results obtained by Pohl [15]. The horizontal displacement is evaluated at D2. Note that Fig. 5a presents teeth in the softening branch, which occurs by the stiffness degradation of each element. For the fine mesh, these teeth are smoother. Figures 5a and 5b also demonstrate that the adopted continuation method can perform the analysis with snap-back phenomena.

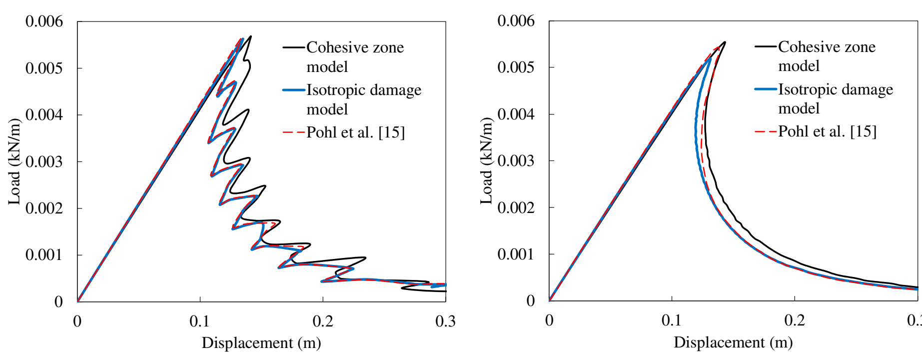

(a) (b)

Figure 5. Load-displacement curve for (a) coarse and (b) fine mesh

The second example considers the experimental results of an L-shaped concrete panel, as depicted in Fig. 6. The experimental program is described by Winkler et al. [18]. This example is proposed to investigate the different criteria and damage evolution laws. The material properties are $E = 25.85$ GPa, $\upsilon = 0.18$, $r_0 = 0.0001044487$ and $G_f = 90.5$ N/m. The fracture energy value used in this work was computed by Oliver et al. [16]. For a linear damage evolution law, the value of r_{max} is calculated according to the expression presented by Pohl et al. [15] using the characteristic length.

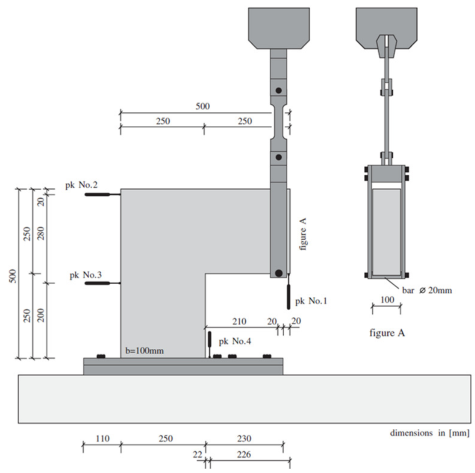

Figure 6. Experimental test setup for the L-shaped panel (Winkler et al. [18])

Figure 7a compares three experimental load-displacement responses developed by Winkler et al. [18] and numerical results using different continuum damage models. Mazars and modified von Mises criteria, as well as linear and exponential damage evolution laws, are adopted in this problem. Additionally, a correction process of the load-displacement curve is adopted, according to Kitzig and Häussler-Combe [22]. They presented how a typical numerical model overestimated the initial branch of this response. The damage constitutive model cannot generate this additional stiffness since it does not affect this branch. This observation indicates that a rigid body rotation in the panel occurred due to a certain elasticity of the support.

Notice that the presented responses showed a softening behavior, as observed in the experimental test. Moreover, the constitutive model that combines the damage criterion proposed by Mazars [4] and the damage law proposed by Kurumatani et al. [5] could predict the peak load of the structure. The damaged region for this model is depicted in Fig. 7b. Nevertheless, the numerical softening branches are different compared to the experimental results. Additionally, note that the numerical models that used the modified von Mises criterion presented a peak load lower than the models that adopted the Mazars criterion. This difference is due to the elastic domain in the region with two positive principal stress (considering plane stress condition) being lower in the modified von Mises criterion than in the Mazars criterion.

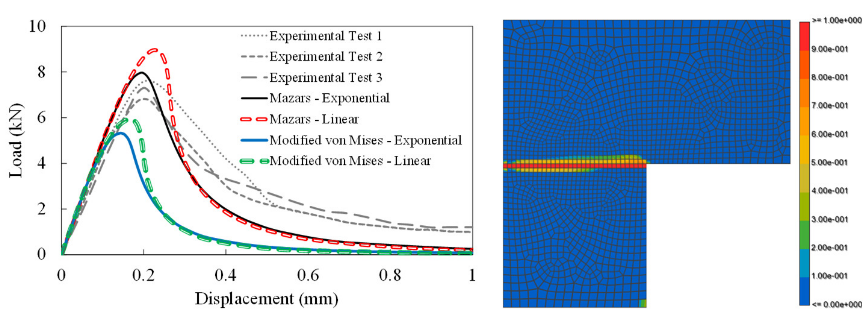

(a) (b)

Figure 7. Numerical results: (a) load-displacement curves considering different combinations of damage criteria and damage evolution laws and (b) damaged region

5 Conclusion

This work presents numerical simulations of fracture propagation using the isotropic damage and cohesive zone models. The continuum damage modeling can be performed considering several damage criteria and damage evolution laws, whose application depends on the type of engineering problem. Numerical examples demonstrate that the cohesive zone and isotropic damage models can describe the initiation and fracture propagation in quasi-brittle materials. Also, the continuum damage model could adequately describe the global behavior of the structure observed in the experimental test. The combination of the damage criterion proposed by Mazars [4] and the exponential damage evolution law proposed by Kurumatani et al. [5] could predict with reasonable accuracy the experimental peak load, different from the other damage criteria and law combinations.

Acknowledgements. This study was financed by the Coordenação de Aperfeiçoamento de Pessoal de Nível Superior – Brasil (CAPES), Conselho Nacional de Desenvolvimento Científico e Tecnológico – Brasil (CNPq) Grants 132421/2019-4, 142461/2020-2 and 309384/2019-2, FAPERJ Grant E-26/202.928/2019, and Tecgraf Institute – PUC/Rio.

Authorship statement. The authors hereby confirm that they are the sole liable persons responsible for the authorship of this work, and that all material that has been herein included as part of the present paper is either the property (and authorship) of the authors, or has the permission of the owners to be included here.

References

[1] Van Mier, Jan G. M.Concrete Fracture: A Multiscale Approach. 1ª. ed. New York: CRC Press Taylor & Francis Group, 2013. 331 p.
[2] Wight, K.W, Macgregor, J.G. Reinforced Concrete – Mechanics and Design. Pearson Education, Upper Saddle River, NJ, 6ª ed, 1157p., 2012.
[3] Lemaitre, Jean. How to use damage mechanics. Nuclear Engineering and Design, v.80, n.2, p.233–245, 1984.
[4] Mazars, J. Mechanical Damage and Fracture of Concrete Structures. Advances in Fracture Research, v.4, p.1499–1506, 1982.
[5] Kurumatani, Mao; Terada, Kenjiro; Kato, Junji; Kyoyan, Takashi; Kashiyama, Kazuo. An isotropic damage model based on fracture mechanics for concrete. Engineering Fracture Mechanics, v.155, p.49–66, 2016.
[6] Oliver, J; Cervera, M; Oller, S. Isotropic Damage Models and Smeared Crack Analysis of Concrete. Computer Aided Analysis and Design of Concrete Structures, Vols 1 and 2, n.January, 1990.
[7] De-Pouplana, Ignasi; Oñate, Eugenio. Combination of a non-local damage model for quasi-brittle materials with a mesh-adaptive finite element technique. Finite Elements in Analysis and Design, v. 112, p. 26–39, 2016.
[8] De-Pouplana, Ignasi. An Isotropic Damage Model for Geomaterials in the KRATOS Framework. 2015. 126 f. Thesis (master's) - Camins School, UPC Barcelonatech, 2015.
[9] J. Simo, J. C.; JU, J. W. Strain-and stress-based continuum damage models-I. formulation. International journal of solids and structures, 23(7):821–840, 1987.
[10] Nguyen, Vinh Phu. Discontinuous Galerkin/extrinsic cohesive zone modeling: Implementation caveats and applications in computational fracture mechanics. Engineering Fracture Mechanics, v.128, n.C, p.37–68, 2014.
[11] Mejia, Eleazar Cristian Sanchez; Paullo Muñoz, Luis Fernando; Roehl, Deane. Discrete fracture propagation analysis using a robust combined continuation method. International Journal of Solids and Structures, v. 193–194, p. 405–417, 2020.
[12] De Vree, J. H.P.; Brekelmans, W. A.M.; Van Gils, M. A.J. Comparison of nonlocal approaches in continuum damage mechanics. Computers and Structures, v. 55, n. 4, p. 581–588, 1995.
[13] Bažant, Zdeněk P; Carol, Ignacio; Caner, Ferhun C; Adley, Mar D.; Akers, Stephen A. Microplane Model M 4 for concrete. I: Formulation with Work-conjugated Deviatoric stress. Journal of Engineering Mechanics, v. 126, n. 9, p. 944–953, 2000.
[14] Caner, Ferhun C.; Bažant, Zdeněk P. Microplane model M7 for plain concrete. II: Calibration and verification. Journal of Engineering Mechanics, v. 139, n. 12, p. 1724–1735, 2013.
[15] Pohl, Tanja; Ramm, Ekkehard; Bischoff, Manfred. Adaptive path following schemes for problems with softening. Finite Elements in Analysis and Design, v. 86, p. 12–22, 2014.
[16] Oliver, J.; Huespe, A,; Pulido, M. D. G.; Blanco, S. Computational modeling of cracking of concrete in strong discontinuity settings. Journal International: Computers and Concrete, v. 1, n. 1, p.61-76, 2004.
[17] Moreira, José Fabiano Araújo; Evangelista Junior, Francisco. Continuous and discontinuous modeling of failure for quasi-brittle materials. Proceedings of the XL Ibero-Latin-American Congress on Computational Methods in Engineering. Natal, RN. November 11-14, 2019.
[18] Winkler, B.; Hofstetter, G.; Niederwanger, G. Experimental verification of a constitutive model for concrete cracking. Proceedings of the Institution of Mechanical Engineers Part L: Journal of Materials: Design and Applications, v. 215, n. 2, p. 75–86, 2001.
[19] Paullo Muñoz, Luis Fernando; Roehl, Deane. A Continuation method with combined restrictions for nonlinear structure analysis. Finite Elements in Analysis and Design, v. 130, n. April, p. 53–64, 2017.
[20] Guitiérrez, Miguel A. Energy release control for numerical simulations of failure in quasi-brittle solids. Communications in Numerical Methods in Engineering, v. 20, n. 1, p. 19–29, 2004.
[21] Mendes, Carlos A. T.; Gattass, Marcelo; Roehl, Deane. The Framework – An innovative framework for the development of multiphysics and multiscale simulations.In: VII EUROPEAN CONGRESS ON COMPUTATIONAL METHODS IN APPLIED SCIENCES AND ENGINEERING. Crete Island: Greece, 2016. p. 1-9.
[22] Kitzig, Mirko; Häussler-Combe, Ulrich. Modeling of plain concrete structures based on an anisotropic damage formulation. Materials and Structures/Materiaux et Constructions, v. 44, n. 10, p. 1837–1853, 2011.